RESEARCH

A comprehensive study of air jet impingement on curved surfaces: experimental analysis and correlation development

Sana Ansari[1] · Laxmikant Dhruw[1] · Hardik B. Kothadia[1] · Arun Kumar R[1]

Abstract

The study focused on examining the area-averaged heat transfer characteristics of an air jet impinging on a concave surface. The experiments involved varying the Reynolds number (Re) within the range of 10,000 to 75,000, while adjusting the jet-to-plate distance from 3 to 20 times the jet diameter (d). The experimental setup included a jet with a diameter of 11.5 mm, and concave surfaces with curvature radii of 218 mm (Curvature ratio (Cr) = 0.026) and 281 mm (Cr = 0.021) were used. A detailed investigation was conducted using Infrared Thermography to measure the average Heat Transfer Coefficient (HTC) of jet impingement on these concave surfaces. The aim was to assess the impact of surface curvature on heat transfer at different locations from the impingement point. Additionally, the research compared the heat transfer effects in circular and square impingement regions that were identical in radial span and area ratios. It was observed that the area-averaged Nusselt number (Nu) generally increased with a higher Re and a lower jet-to-plate distance ratio (z/d). A maximum average Nu increase is observed for Cr = 0.026 when the mass flow rate is from 10,000 to 75,000. Increasing the curvature is an effective approach to provide localized cooling. A correlation comparison was also conducted, and a new empirical correlation has been proposed. This correlation works effectively across various ranges of Re, z/d, Cr, and radial position (r/d) with a deviation of less than ± 11%.

Nomenclature

Aj	Area of Jet (m^2)
A_r	Area ratio
As	Square Area (m^2)
Ac	Circular Area (m^2)
Ap	Surface area of Plate (m^2)
b	Height of slot nozzle (m)
Cr	Curvature ratio (d/D)
D	Diameter of concave surface (m)
d	Nozzle diameter (m)
d_h	Hydraulic diameter
h	Heat Transfer Coefficient (W/m^2K)
HT	Heat transfer
I	Current (A)
k	Thermal conductivity of air (W/mK)
L	Nozzle length (m)
L_p	Length of plate (m)
m	Mass flow rate (kg/s)
MAD	Mean Absolute Deviation
Nu	Nusselt number
P_m	Perimeter (m)
q^ε_{joule}	Net heat supplied (W/m^2)
q_{nat_c}	Heat flux due to natural convection (W/m^2)
q^ε_{loss}	Heat loss by convection and radiation (W/m^2)
q^ε_{conv}	Convective heat flux transferred by jet flow (W/m^2)
q^ε_{rad}	Heat loss due to radiation (W/m^2)
r	Radial distance from impingement point (m)
RTD	Resistance temperature detector
R	Radius of curvature of concave plate (m)
Re	Reynold number
t	Plate thickness
T_f	Fluid temperature (K)
T_w	Wall temperature (K)
T_a	Ambient temperature (K)
v	Velocity of air jet (m/s)
V	Voltage (V)
w	Width of the slot nozzle (m)

✉ Hardik B. Kothadia
hardikkothadia@iitj.ac.in

Sana Ansari
ansari.4@iitj.ac.in

Laxmikant Dhruw
dhruw.1@iitj.ac.in

Arun Kumar R
arunkr@iitj.ac.in

[1] Department of Mechanical Engineering, Indian Institute of Technology Jodhpur, Jodhpur 342037, India

W	Plate width
z	Nozzle exit to target plate spacing *(m)*

Subscripts

a	Ambient
avg	Average
c	Convection
exp	Experimental
fr	Front
bk	Back
f	Fluid

Greek symbol

σ	Stefan-Boltzmann constant
α	Thermal diffusivity (m^2/s)
υ	Kinematic viscosity of air (kg/m.s)
μ	Dynamic viscosity, (Nm/s^2)
ρ	Density (kg/m^3)

1 Introduction

The study of heat transfer from jet impingement on curved surfaces has been the subject of extensive research for many years. It offers an efficient means to enhance convective processes due to the high rates of heat and mass transfer that can be achieved. Jet impingement finds numerous industrial applications, including the annealing and tempering of metals, cooling of heated plates and rods, glass manufacturing, furnace heating, drying in the food [1], paper, film, and textile industries, cooling of electronic components [2], combustion chamber cooling [3], cooling of marine heat exchangers, freezing of tissues in cryosurgery, and anti-icing systems of aircraft wings [4]. Impinging jets are commonly employed when a high rate of heat transfer (HT) is required. Understanding the factors influencing heat transfer rates is crucial for optimizing the design of these systems. When a jet strikes a surface, the heat transfer rate is influenced by several complex parameters, including the Reynolds number (Re), Prandtl number (Pr), Nusselt number (Nu), dimensionless jet-to-plate distance (z/d), and radial distance from the impingement point (r/d). Factors such as flow confinement, nozzle exit turbulence intensity, nozzle geometry, jet temperature dissipation, target plate inclination, surface roughness, and curvature also significantly impact the process.

Jet impingement has been utilized on both concave [5, 6] and convex curved surfaces in various engineering applications. For instance, concave surfaces are used in turbine rotor blade leading edge cooling, aerofoil leading edge heating for anti-icing purposes [7, 8] and vertical and/or short take-off and landing (V/STOL) aircraft aerodynamics [9]. Lee et al. [10] investigated a long round jet impinging on a concave plate with varying curvature

ratios (Cr = 0.089, 0.056, and 0.034) and mass flow rates ranging from 11,000 to 50,000. They noticed that the Nu at the impingement point increases with higher curvature. Bu et al. [8] explored the heat transfer coefficient of a jet impinging on a wing's leading edge with variable curvature. They analyzed the effect of nozzle-to-surface distance, jet Re, and circumferential distribution on the local Nu. Zhou and Dong [11] numerically investigate the impact of jet diameter variation on the cooling performance of single row jet impingement when the negative influence of cross flow is considered in a semicircular target channel with a single exit. Results of investigations are carried out under five jet diameter arrangements and three jet Reynolds numbers ranging from 10,000 to 20,000. To quantify the development of cross flow, the mass velocity ratio of the impinging jet to the cross flow is utilised. Öztekin et al. [12]. conducted both experimental and computational studies on a slot jet impinging on a concave surface. They observed that the average Nu increases as the separation between the impinging jet and the target surface reduces.

The literature review on jet impingement over concave surfaces is concisely summarized in Table 1, which provides an overview of the geometrical dimensions of the test plates and nozzles, boundary conditions, flow rates, average Nusselt number (Nu) correlations, and key findings from existing research. As indicated in Table 1, the parametric studies primarily focus on small curvature ratios (Cr). It is noteworthy that all the reviewed literature investigates the average heat transfer (HT) distribution, yet there is a lack of studies observing the area-averaged Nu distribution. Additionally, there appears to be an absence of research comparing the effects of varying shapes of the impinging plate area on HT distribution over concave surfaces. There are currently only three available correlations that can predict average Nusselt numbers as a function of z/d, Re, and d/D. These correlations do not account for the heat transfer area (r/d). As a result, new correlations have been introduced to predict area averaged Nusselt numbers, taking into consideration the heat transfer area. The study of area-averaged HT distribution is important for optimizing design, enhancing cooling systems, selecting suitable materials, understanding temperature gradients, and advancing research in various fields related to thermal energy transfer. This knowledge has a practical application in industries and technologies where efficient heat management is essential.

The present study was undertaken to investigate the effect of relative curvature on surface heat transfer. The area average temperature and Nu distribution are measured for a round jet impinging perpendicularly on a concave surface. The relative curvature (Cr) varies by changing the surface diameter. Temperature distributions were

extensively quantified by infrared thermography. The average HT characteristics in a stagnation, transition, and free wall jet region were studied. The objective of this study is to investigate the jet-to-surface distance, Cr and Re on area-averaged HTC. The study focused on the effect of a jet striking a heated, curved plate on a specific area. A novel correlation has been established, which agrees well with the present experimental data and is applicable across the entire range of Re, r/d, and d/D.

2 Methodology

2.1 Test setup

The experimental apparatus illustrated in Fig. 1 is used to investigate the HT and fluid dynamics. The primary apparatus consists of an air supply, a concave plate, and a nozzle. Air is supplied by a compressor capable of maintaining consistent pressure. It is facilitated by a pressure controller and monitored using a pressure gauge. An air compressor provides the necessary air. To maintain consistent pressure, an air compressor is equipped with a pressure controller. A pressure gauge is fitted to it to display the pressure of the tank. The pressure tank, with a capacity of 6 m^3 and a maximum pressure of 30 bar, is integrated with an orifice meter to measure airflow. A control valve regulates this flow. The nozzle, with a length of 1 m and an internal diameter of 11.5 mm, serves as a circular air jet impinging on the concave surface. The length-to-diameter ratio (L/d) of 87 ensures a fully developed flow for Re between 10,000 and 75,000. The setup includes a precision vice that holds the plate firmly, allowing for adjustments in both transverse and axial directions. This adjustability is key for modifying the distance and position of the jet impingement on the plate.

The concave surface used in the experiment is symmetric and constructed from SS 304, measuring 600 mm × 300 mm with a thickness of 0.1 mm. It features two radii of curvature: 218 mm (d/D = 0.026) and 281 mm (d/D = 0.021). This curved plate is firmly held between two vertically positioned copper (Cu) busbars. The minimal thickness of the sheet reduces the effect of lateral conduction, resulting in a uniform heat flux condition. It can be confirmed through 1D energy equilibrium analysis [17]. The Cu busbars are connected to an AC power supply (Elenco XP–625). The output is adjusted with the help of an autotransformer. The voltage drop across the plate is measured using a Voltmeter (METRA Hit 2+) with a range of 0 to 20V and an uncertainty of 1%. The current is measured using an Ammeter (Metravi DT-125) with an uncertainty of 0.5% and a measuring range of 0 to 300 amperes. Temperature data is captured

using an IR camera (Testo 890) focused on the convex surface of the plate, which is coated with black paint having an emissivity of 0.92. IR camera measures the temperature of the plate depending on emissivity. Additionally, a Resistance Temperature Detector (Tempsens) having a measuring range up to 150 °C is utilized to ascertain the fluid temperature. The IR camera, with a resolution of 480 × 640 pixels, records the temperature across the heated plate. It presents the data as a planar image captured from the convex side. To convert this temperature data into the actual cylindrical geometry of the surface, the below equation [18] is used.

$$r = R \times \varnothing = \text{R} \times \sin^{-1}\frac{X}{R} \tag{1}$$

where R denotes the radius of curvature, r denotes the length along the curvature of the plate, $\varnothing$ is the angle created between 2 points along the curvature of the plate, and X denotes planar length.

2.2 Data reduction

Once the steady-state condition has been attained, the spatial temperature variation across the convex surface is measured by an IR camera. The temperature of an air jet can be determined through RTD. The HTC is evaluated using the Nusselt number which can be determined from Eq. (2). h is the convective HT coefficient, which is governed by Nu:

$$Nu = \frac{hd}{k} \tag{2}$$

$$h = \frac{q''conv}{T_w - T_j} \tag{3}$$

Tw denotes surface temperature, Tj denotes jet temperature, and q"conv denotes net heat flux.

As indicated in Eq. (4) the balance heat flux [5, 19, 14] is calculated by removing the lost heat from supplied heat flux.

$$q''_{conv} = q''_{joule} - q''_{loss} \tag{4}$$

$$q''_{loss} = q''_{nat\_c} + q''_{rad\_bk} + q''_{rad\_fr} \tag{5}$$

$$q''_{joule} \times A = VI \tag{6}$$

According to Eq. (5) the total heat loss is equal to convection HT from the rear and radiation losses from the front and back sides of a heated plate. Churchill and Chu [20] gave an empirical correlation for losses due to natural convection. Radiation loss is calculated by Stefan Boltzmann equation as mentioned in Eq. (10)

Table 1 Average Nu correlations for a concave surface

Author (Year)	Radius of Curvature	Nozzle geometry (Dimension)	Re / Average Nu correlation	z/d	Cr	Findings
Gau and Chung [13] (1991)	R = 80 mm	**Slot** (w = 3.5 mm, 6 mm, 15 mm, and 20 mm)	6,000 to 350,000 $Nu_{avg} = 0.251\,Re^{0.68}\,(D/w)^{-0.38}(z/b)^{0.15}$ $2 \le z/w \le 8$ $Nu_{avg} = 0.394\,Re^{0.68}\,(D/w)^{-0.38}(z/b)^{-0.32}$ $8 \le z/w \le 16$ $6{,}000 \le Re \le 35{,}000$ and $8 \le D/w \le 45.7$	2 to 16	0.022 to 0.125	HT increases as the surface curvature of the concave surface increases. This characteristic is illustrated by the development of Taylor Görtler vortices. It improves HT over the surface and increases momentum transfer in the flow.
Fenot et al. [14] (2008)	R = 50 mm	**Circular** (d = 10 mm, 15 mm, and 20 mm)	10,000 to 23,000 $Nu_{avg} = 0.042\,Re^{0.72}\,(d/D)^{-0.085}(z/d)^{-0.06}$ $10{,}000 \le Re \le 23{,}000$, $2 \le z/d \le 5$ and $0.1 \le d/D \le 0.2$	2 to 5	0.1 to 0.2	The Nu in the impingement zone grows slightly as the curvature increases. Curvature causes the jet's flow to be constrained, which has two consequences: stagnation of the adiabatic wall temperature and a reduction in the Nu distribution.
Zhou et al. [15] (2017)	R = 50 mm and 100 mm	**Circular** (d = 2 mm)	27,000 to 130,000 $Nu_{avg} = 0.0065\,Re^{0.638}\,(d/D)^{-0.183}\,(z/d)^{0.0312}$ $Nu_{avg} = 0.014\,Re^{0.638}\,(D/L)^{0.183}\,(z/d)^{0.0312}$ $54{,}000 \le Re \le 86{,}000$, $5 \le z/d \le 15$ and $0.67 \le D/L \le 1.33$	3.3 to 30	0.005 to 0.03	Increasing the distance between the nozzle and the surface increases the average HT over the surface (increasing jet diameter). With a constant jet diameter, the average Nu decreases as the distance between the nozzle and surface increases.
Hadipour and Zargarabadi [16] (2018)	R = 120 mm	**Circular** (d = 24 mm)	10,000 to 35,000 $Nu_{avg} = 0.11\,Re^{0.63}\,(z/d)^{-0.54}$ $0.1 \le z/d \le 0.4$ $Nu_{avg} = 0.5\,Re^{0.54}\,(z/d)^{-0.14}$ $1.0 \le z/d \le 4.0$	0.1 to 4	0.1	Jet with a small nozzle to surface distance (z = 0.1d, 0.2d and 0.4d) have high Nu distribution in comparison with the surface with a large nozzle to surface distances (z = d, 2d and 4d).

Fig. 1 Test system: 1) Air compressor. 2) Storage container. 3) The Pressure gauge. 4) Control valve. 5) Orifice meter. 6) Impinging jet configuration. 7) Traversal system. 8) Curved surface configuration. 9) Power source. 10) IR Camera. 11) Multimeter. 12) Data acquisition system
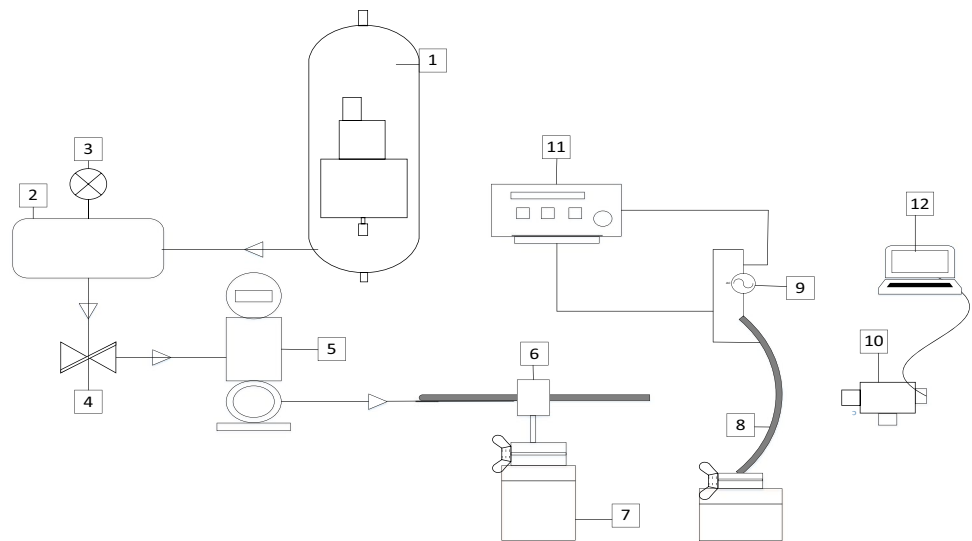
$$Ra_L = \frac{g\beta(T_w - T_f)L_c^3}{\alpha.\nu} \tag{7}$$

where Ra_L Rayleigh Number for vertical plate which ranges from $10^4 - 10^{13}$

$$L_c = \frac{A}{Pm} \tag{8}$$

$$q_{nat\_c} = h_{nat\_c} \cdot (\triangle T), \text{ where } \triangle T = T_w - T_f \tag{9}$$

$$q_{rad_{fr}} \text{ or } q_{rad_{bk}} = \sigma.\varepsilon \cdot (T_w^4 - T_f^4) \tag{10}$$

The parameters of an impinging jet, such as density, viscosity, and thermal conductivity at fluid jet temperature, are measured at the nozzle exit. The non-dimensional variables that affect jet impingement HT include fluid thermophysical properties, such as the Reynold number, and Prandtl number, as well as various geometrical and flow variables.

The area average HTC in stagnation, free jet, and wall jet regions on a concave surface has been investigated. Figure 2 depicts the test plate schematically and shows the stagnation point, location of the square and circular areas, and dimension of the test plate. The stagnation point is considered the origin. After striking the plate, the jet flows in all directions, radially parallel to the concave surface. The letter 'r' represents the radial length from the origin, which increases radially along the length. The average Nu and temperature are calculated over the square and circular areas. Over the plate, 5 regions of square and circle with the same radial length are indicated to analyze the area average HT. It is denoted as A1, A2, A3, A4, and A5 with A1 ($0 < r/d < 2.17$), A2 ($0 < r/d < 4.35$), A3 ($0 < r/d < 6.52$), A4 ($0 < r/d < 8.7$), and A5 ($0 < r/d < 10.87$).

The Nu and Re uncertainties were evaluated using the approach proposed by Kline and Mc Clintock [21]. The uncertainty of fluid temperature measurements is ± 0.3 °C. The uncertainty in heat flux is about $\pm 2.83\%$. The power supply has an uncertainty of $\pm 1.32\%$, while the IR camera has an uncertainty of ± 0.6 °C. $\pm 1.5\%$ relative uncertainty characterizes the mass flow controller. The uncertainty in the Reynolds number and Nusselt number, respectively, is around $\pm 2.5\%$ and $\pm 7.73\%$.

The procedure to calculate uncertainty in heat transfer is stated below:

$$U_{\dot{Q}} = \sqrt{\left((U_Q)_{total}\right)^2 + \left((U_Q)_{loss}\right)^2} \tag{11}$$

$$\left(U_{\dot{Q}}\right)_{total} = \sqrt{\left(\frac{\delta V}{V}\right)^2 + \left(\frac{\delta I}{I}\right)^2 + \left(\frac{\delta L}{L}\right)^2 + \left(\frac{\delta W}{W}\right)^2} \tag{12}$$

The sample experimental case for uncertainty in heat flux is presented below. A current of 174 Amperes and a voltage of 3 Volts are supplied to the test section. The length and width of the test plate are 600 mm and 300 mm, respectively. The associated uncertainty is:

$$\left(U_{\dot{Q}}\right)_{total} = \sqrt{\left(\frac{0.03}{3}\right)^2 + \left(\frac{0.86}{174}\right)^2 + \left(\frac{0.0015}{0.6}\right)^2 + \left(\frac{0.003}{0.3}\right)^2} \tag{13}$$

$$\left(U_{\dot{Q}}\right)_{total} = 0.0152$$

The uncertainty in total heat flux supplied to test plate $= 0.0112$

$$\left(U_{\dot{Q}}\right)_{loss} = \sqrt{\left(\frac{\delta Q_{loss}}{Q_{loss}}\right)^2 + \left(\frac{\delta L}{L}\right)^2 + \left(\frac{\delta W}{W}\right)^2} \tag{14}$$
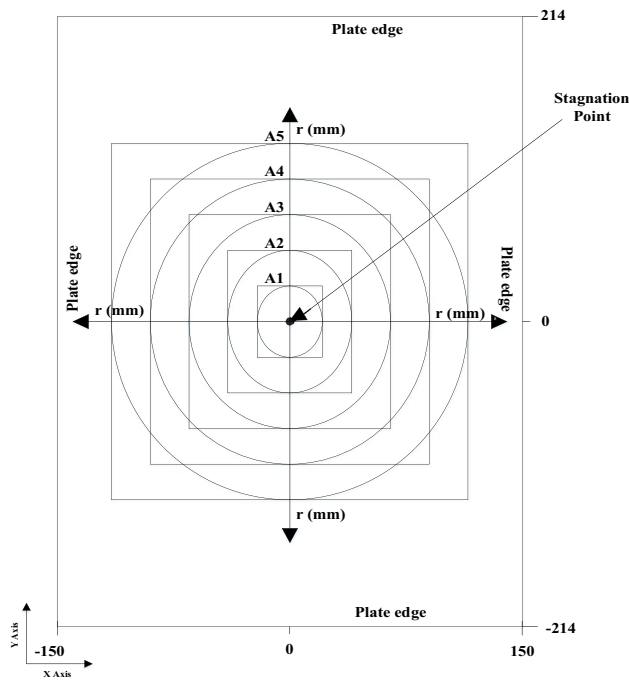
Fig. 2 Area-wise description of target surface

$$(U_{\dot{Q}})_{loss} = \sqrt{\left(\frac{0.334}{13.36}\right)^2 + \left(\frac{0.0015}{0.6}\right)^2 + \left(\frac{0.003}{0.3}\right)^2} \quad (15)$$

The uncertainty in heat loss $= 0.027$

$$(U_{\dot{Q}})_{act} = \sqrt{\left((U_{\dot{Q}})_{total}\right)^2 + \left((U_{\dot{Q}})_{loss}\right)^2} \quad (16)$$

The uncertainty in heat flux is obtained as 2.83%.

The heat transfer coefficient gives maximum uncertainty at minimum wall and bulk fluid temperature difference and for maximum uncertainty in wall and bulk fluid temperature.

$$U_h = \sqrt{\left(\frac{\delta\dot{Q}}{\dot{Q}}\right)^2 + \left(\frac{\delta T_s}{T_s - T_f}\right)^2 + \left(\frac{\delta T_f}{T_s - T_f}\right)^2} \quad (17)$$

The minimum temperature difference is 7.3 °C, the heat flux is 527 W. The uncertainty in heat transfer coefficient is 1.27% and Nusselt number is 7.73%.

3 Results and discussion

3.1 Validation of experimental setup

The result of the experiment is supported by previously published research papers. For Re = 23,000 and at z = 6d, the local Nusselt number has been validated across a flat plate impinged by a jet. Figure 3 illustrates the comparison of

local Nu distribution about the ratio of the radial distance to the nozzle diameter (r/d). According to Katti and Prabhu [22] and Goldstein and Behbahani [23], the variation in HT concerning the plate's radial distance from the impingement point of the jet is anticipated to be well within the recognized deviation range. The local Nu curve obtained from the Katti and Prabhu correlation slightly overpredicts the experimental data in the stagnation region, as shown in Fig. 3. After a stagnation region beyond r/d ≥ 4.3, the curve matches close to the experimental data with an overall deviation less than 21%. The correlation of Goldstein and Behbahani predicts the present result well. It underpredicts the data at a lower r/d. On increasing the plate size, i.e., beyond r/d ≥ 6, the correlation overpredicts the experimental data with a maximum deviation of less than 31%.

3.2 Effect of curvature on wall temperature

The graph depicts an area-averaged wall temperature variation under constant heat flux conditions before and after a jet strikes the concave surface. The temperature of the jet before it struck the plate was 24 ºC, while the wall temperature before the impact was 110ºC. The initial wall temperature was reached under no flow condition, i.e., Re = 0, and the plate was heated uniformly. A consistent pattern is observed on both surfaces: the lowest wall temperature (Tw) is found in the A1 region, while the highest is in the A5 region. This can be attributed to the significantly greater influence of flow intensity in the vicinity of the stagnation zone. When the jet strikes the surface in the stagnation region, fluid flow ceases abruptly. This location kinetic energy is increased due to the abrupt fluid deceleration. The flow is at its greatest strength at the point of stagnation due to the sudden decrease in velocity; this generates a greater impact force, which in turn causes a more substantial decrease in temperature.

Figure 4(a, b) demonstrates the effect of different curvature ratios on the area-averaged wall and jet temperatures at a constant Re, by varying the z/d ratio. As the curvature ratio increases, the average wall temperature also increases. This is due to the confinement effect, in which decreasing the surface diameter of a concave surface increases the average wall temperature. When considering concave surfaces, the difference in wall temperature becomes less pronounced with a higher z/d. This is because the jet spreads out and entrains more ambient fluid, which diminishes the jet intensity. At Re = 35,000, the temperature difference between curvatures in the A1 region is initially 27%, but this reduces to 23% as the z/d is increased from 3 to 12. For Re = 45,000, this variation in the A1 region further declines to only 5% with the same increase in the z/d ratio. Furthermore, the change in wall temperature due to different curvature ratios also diminishes as the area increases. Higher Reynolds numbers enhance the turbulent mixing

Fig. 3 Comparison of the present result with Katti and Prabhu [22] and Goldstein and Behbahani [23] for Re = 23,000, z/d = 6
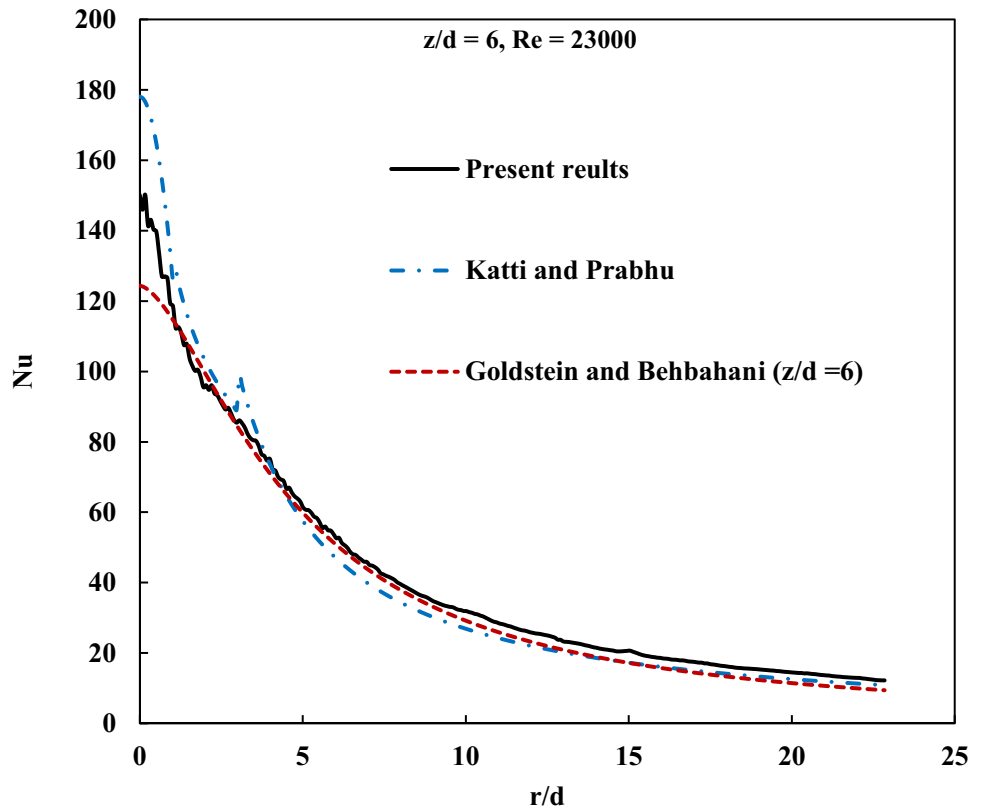

and entrainment, further reducing the temperature disparity across different curvatures. At both Re = 35,000 and 45,000, in the A5 region, the disparity in the Nu between the curvature ratio is minimal, less than 2%, when altering the z/d from 3 to 12. Hence, these observations emphasize that the average variance in wall temperature across different curvatures significantly decreases with an increase in z/d and area.
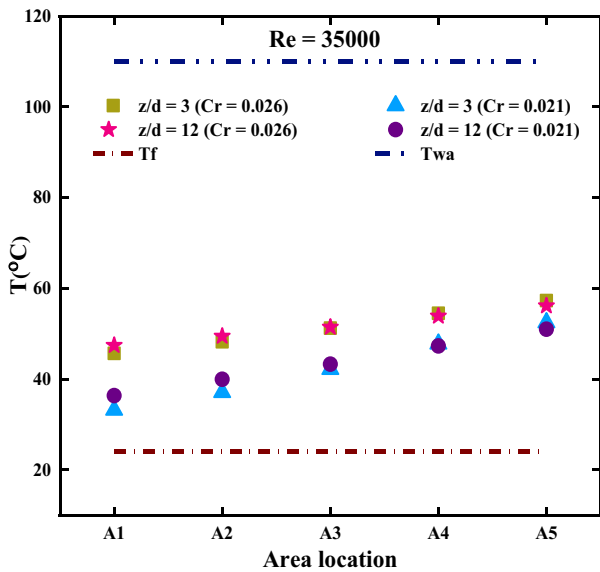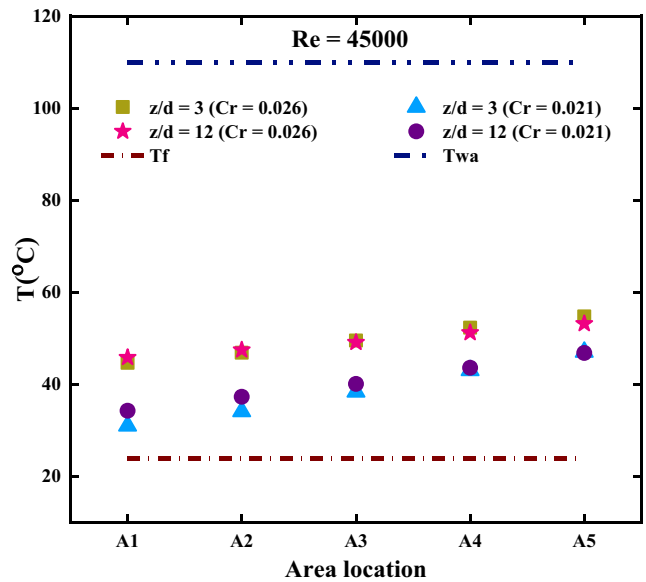
Fig. 4 Effect of curvature ratio on average wall temperature by changing z/d

The influence of surface curvature on the area-averaged wall temperature is explored by varying the mass flow rate, as depicted in Fig. 5(a, b). These figures present the average temperature variation across different surfaces at various area locations of the plate, specifically at z = 6d. For a Re = 10,000, the average wall temperature increases as the curvature decreases. Conversely, for Re values greater than 10,000, an increase in curvature leads to an increase in the average wall temperature. The disparity in wall temperatures across different curvatures becomes less pronounced with higher Re values. It is also observed that from the A1 to A5 region, the rise in wall temperature diminishes with increases in both Re and Cr.

3.3 Effect of jet to plate distance on area-averaged HT

For a Reynolds number (Re) of 10,000, Fig. 6(a) illustrates the effect of z/d on heat transfer (HT). The area-averaged Nusselt number (Nu) is at its maximum near the stagnation region and decreases towards the edges of the plate, specifically in the A5 region (where $0 < r/d < 10.87$). This is because the jet strength decreases as one moves farther from the stagnation region and nearer to the wall jet region. A similar pattern is observed for other values of z/d. In the A1 region ($0 < r/d < 2.17$), the average Nu is highest at z = 3d and lowest at z = 20d. The jet intensity weakens due to the incorporation of ambient fluid into the jet flow, leading to a decrease in heat transfer with increasing z/d. Approaching the A4 region, Nu converges

and becomes constant in the A5 region. This indicates that increasing the plate size beyond a certain r/d ratio does not further affect heat transfer. This trend is consistent across different Reynolds numbers. The area-averaged Nu increases with an increase in Re. The highest area-averaged Nu is observed in the A1 region at z = 6d for Re = 75,000, as depicted in Fig. 6(f).

3.4 Effect of jet Re on area-averaged HT

The distribution of area average Nu at different regions over the concave surface for different Re is depicted in Fig. 7(a)–(d). The average Nu increases with increasing Re. This is attributed to the higher energy and momentum imparted by a jet with greater Re near the impingement region. This is because a jet with a higher Re imparts more energy and momentum near the impingement region. Additionally, in the wall jet zone, higher Re contributes to the formation of Taylor-Görtler vortices [15], leading to increased turbulence intensity and velocity. This enhancement accelerates the heat transfer (HT) rate along the chordwise direction, covering the entire surface. Although the magnitude of Nu decreases when moving from the A1 to the A5 region, the profiles do not coincide. It is also noted that, regardless of the z/d ratio, the relative change in area-averaged Nu in the A5 region for Re = 75,000 and 10,000 remains. This observation demonstrates that the Reynolds number significantly influences heat transfer, even as one approaches the edge of the plate. Furthermore, the location of the maximum average HT is dependent on both the flow rate and the jet-to-plate spacing (z/d), as well as the ratio of Cr.
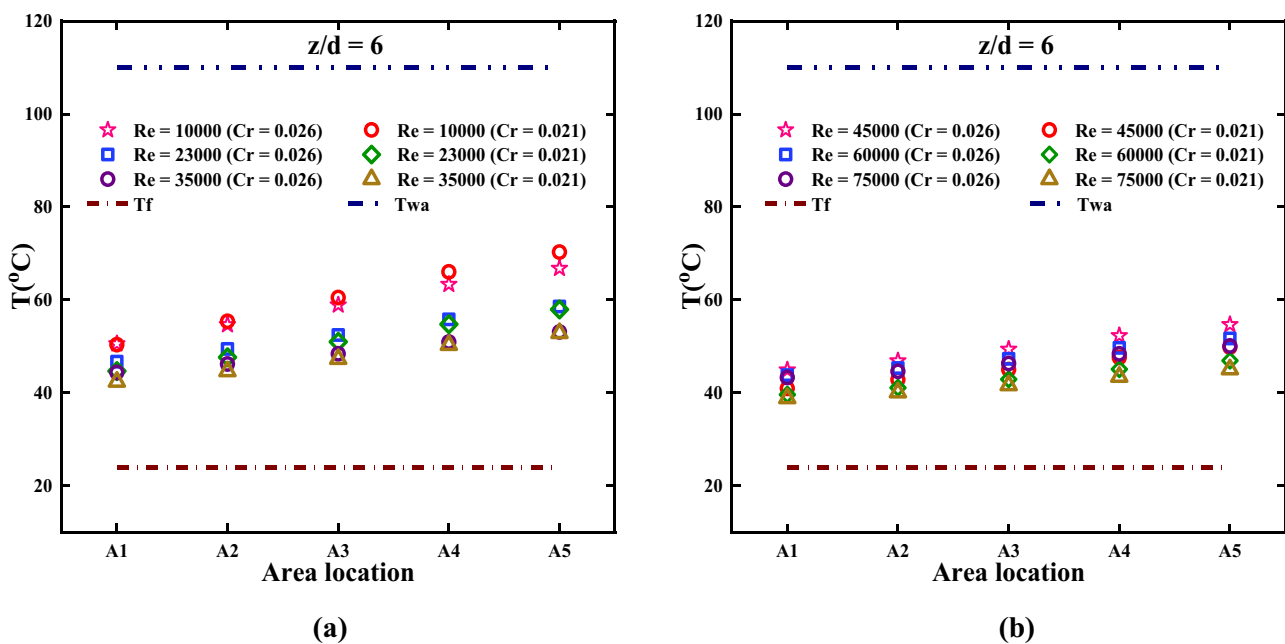

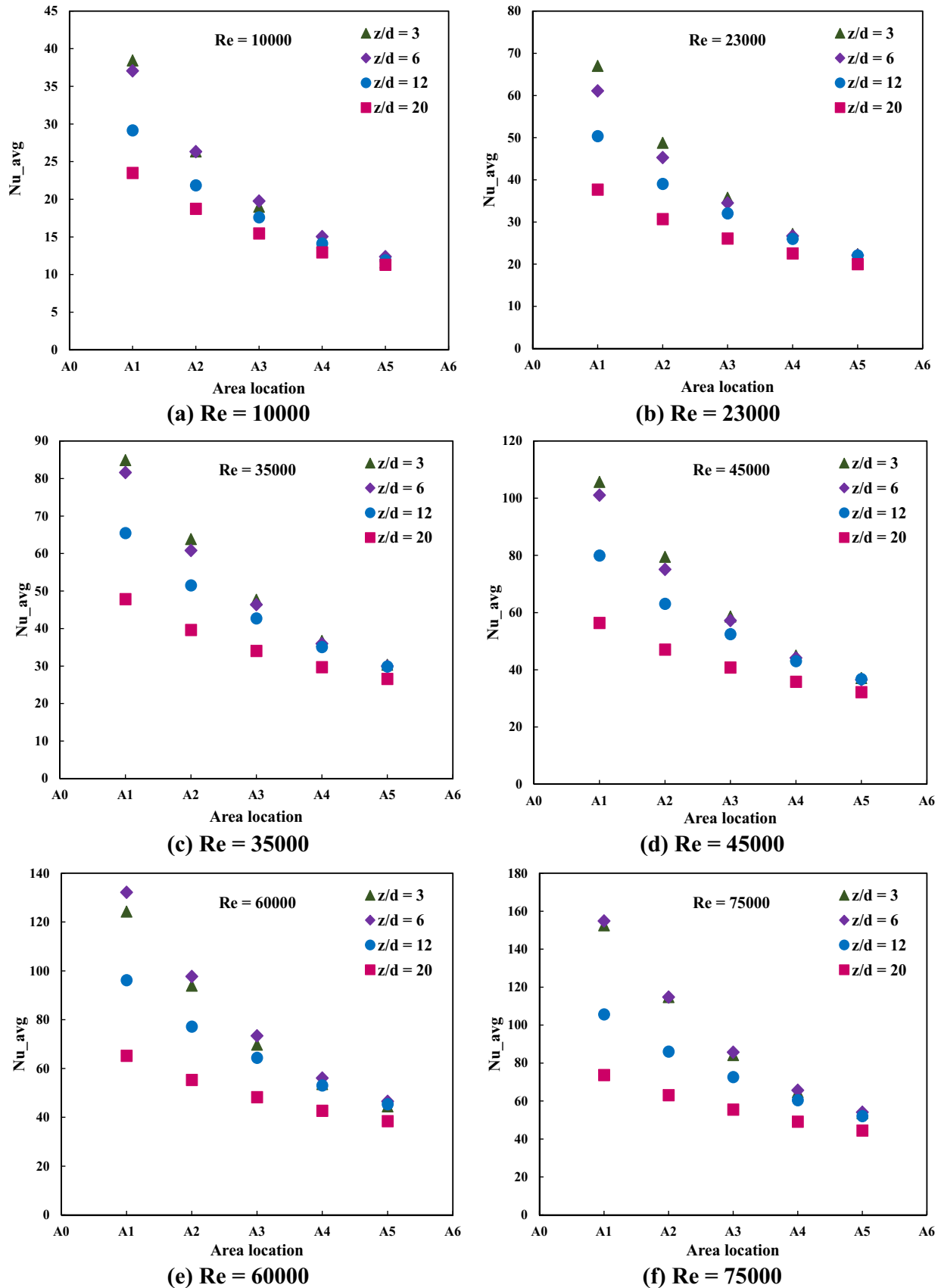Fig. 5 Effect of curvature ratio on average wall temperature with Re

Fig. 6 Area averaged Nu at different locations of the plate by varying z/d for Cr = 0.021
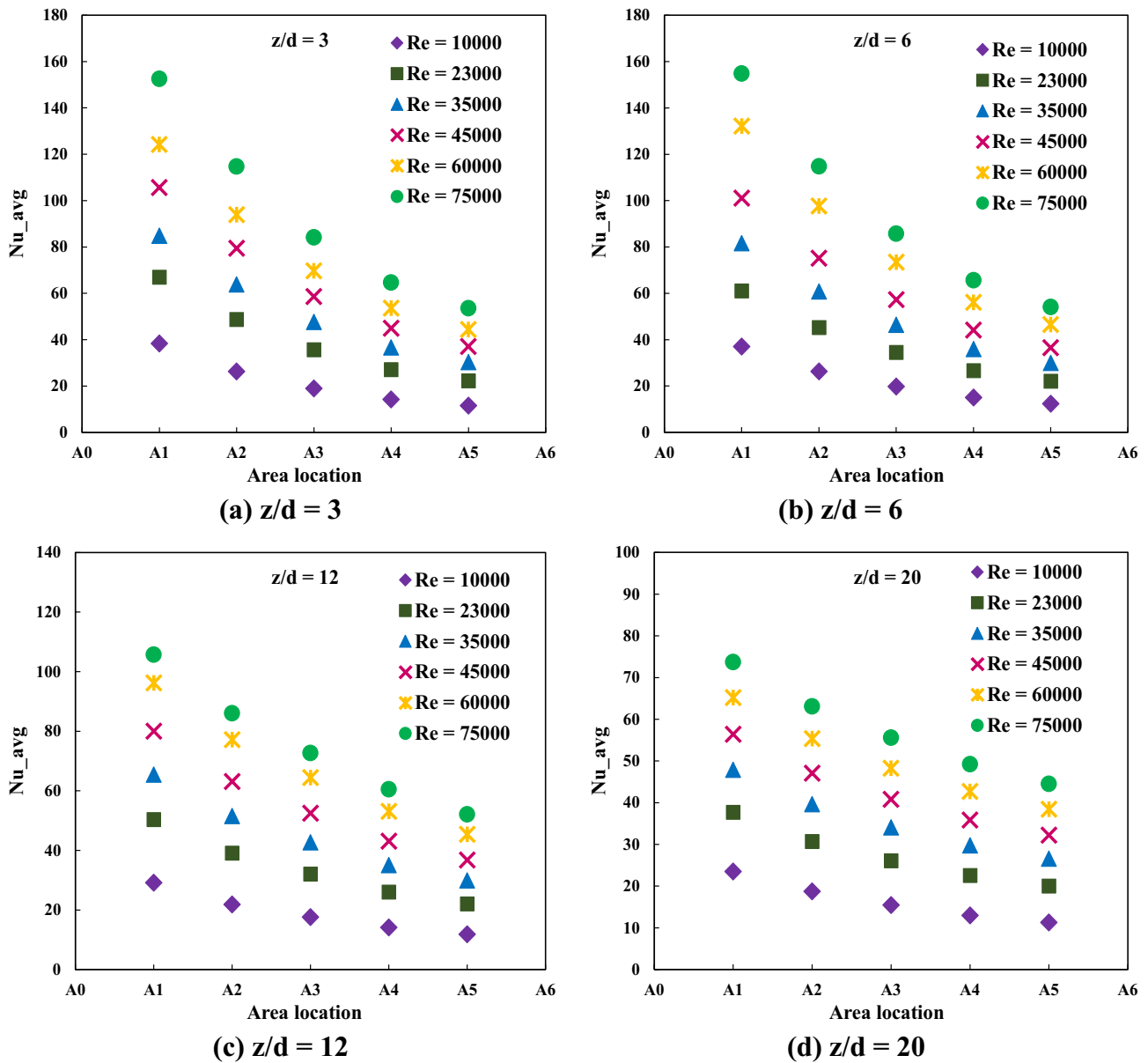
Fig. 7 Distribution of area-averaged Nu by varying Re for Cr = 0.021

3.5 Comparison of area-averaged Nu in circular and square sections

Most commercial impinging plate designs predominantly utilize circular, rectangular, or square shapes due to their cost-effectiveness, simplicity of construction, speed of fabrication, and compatibility with various layouts. This research aims to determine the effects of these shapes on the heat transfer coefficient (HTC). In analyzing infrared (IR) images, we compare the area of circular and square sections that have identical radial lengths. When transforming the planar image of a convex surface into a cylindrical geometry, the square and circular areas in IR images are converted into rectangles and ellipses, respectively, with recalibrated dimensions in pixel terms. As shown in Fig. 2, five square and circular sections have been marked on the heated plate to cover the maximum area. The stagnation point is considered the origin, and the jet movement along the radial length towards the edge of the plate is analyzed.

Figure 8 depicts the average Nusselt number distribution for two sets of Re (35,000 and 75,000) and z/d (6 and 20). For Re = 35,000 and z = 6d, the magnitude of Nu in the circular section exceeds that in the square section at any radial distance, as illustrated in Fig. 8(a). This difference in Nu between circular and square sections increases with r/d. A similar trend is observed for Re = 75,000 and
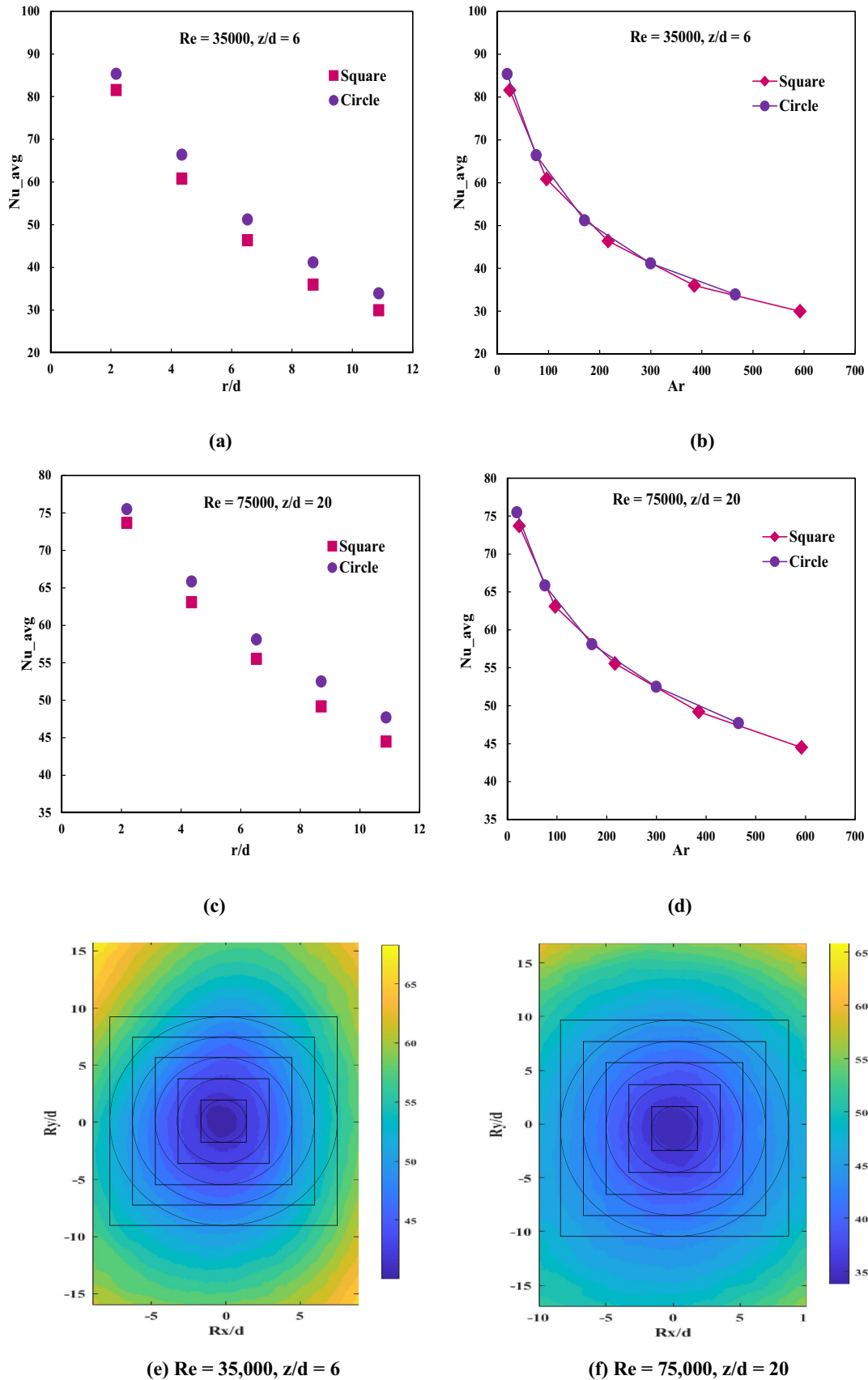
(a)

(b)

(c)

(d)

(e) Re = 35,000, z/d = 6

(f) Re = 75,000, z/d = 20

Fig. 8 Average Nu distribution and temperature contour for square and circular area locations over the heated plate

z = 20d, as seen in Fig. 8(c). It is important to note that for the same radial length, the square section occupies a larger area than the circular section. Since the area is inversely related to the heat transfer coefficient, the jet cooling for the circular section will transfer more heat than the square section for the same radial span.

The variation of area-averaged Nu is plotted against the area ratio in Fig. 8(b) and (d). Interestingly, the data trends for the circular and square sections are similar. At the lowest area ratio, the circular section transfers more heat than the square section. As the area ratio increases, the difference in heat transfer for both sections remain nearly the same, and the data for both curves overlap. Consequently, both shapes provide the same heat transfer for the same area ratio. This occurs because, at the same radial length (r/d), the circular section has a slightly lower area ratio than the square section. The ratio of the circular area to the jet area (Ac/Aj) is less than that of the square area to the jet area (As/Aj), allowing the jet to cover a smaller area and thus transfer heat more efficiently in the circular section. However, the variation in heat transmission is relatively minor when considered from a broader perspective.

The temperature contours on the plate with two different shaped areas, represented as an ellipse and a rectangle, are depicted in Fig. 8(e) and (f). Both areas have the same radial length but different sectional areas. The circumference of the ellipse area meets the edge of the rectangle area, maintaining the same radial length. The average temperature on the plate for Re = 35,000 at z = 6d is 56.69 °C,

while it is 46.84 °C for Re = 75,000 at z = 20d. This indicates that a jet-to-plate distance of 20d with higher Re results in a smaller temperature gradient, leading to a faster heat transfer rate.

3.6 Effect of curvature on area average Nu

This analysis examines the impact of curvature ratio on area average Nu distribution by varying z/d and Re along a concave surface. Generally, the Nu value demonstrates a monotonic decline, starting from its peak at r/d = 2.17 and reaching its lowest point at r/d = 10.16. Results show that the distributions are very close to each other. Specifically, the distribution of Nu along the concave surface for Cr of 0.021 and 0.026, with varying z/d, is depicted in Fig. 9(a, b). A significant decrease in Nu is observed with increasing z/d values, attributed to the rapid decay of jet centerline velocity. At Re = 23000 and z/d = 6, the difference in Nu for a curvature ratio at r/d = 2.17 is 7%, which diminishes to 5% at r/d = 10.9. It is primarily due to the stabilizing and homogenizing influences of boundary layer growth, reduced local velocity gradients, and increased mixing of the jet with the surrounding fluid. In contrast, at a higher Re of 45000, the Nu variation between different curvatures is 5% at r/d = 2.17. However, at z/d = 20, the Nu variation between the two curvatures reduces to less than 2%, regardless of the r/d value. Hence, irrespective of the curvature ratio, the higher z/d has a very minimal effect on the area average Nu distribution.
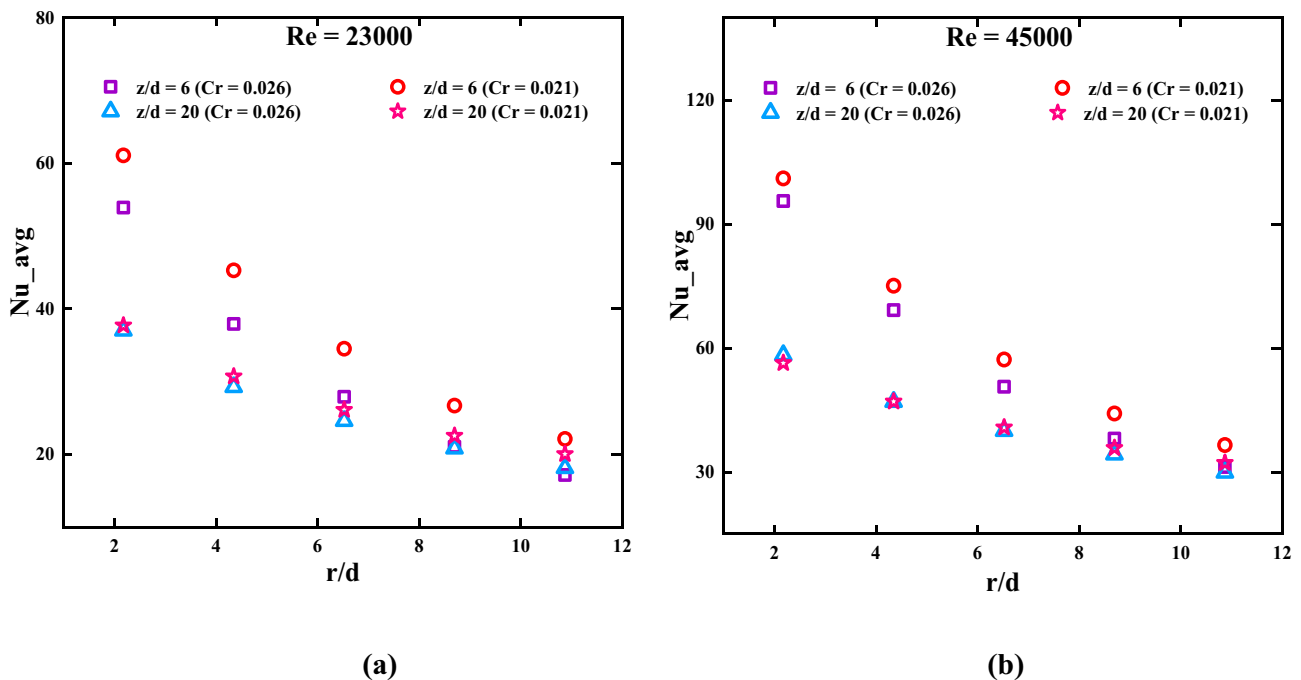

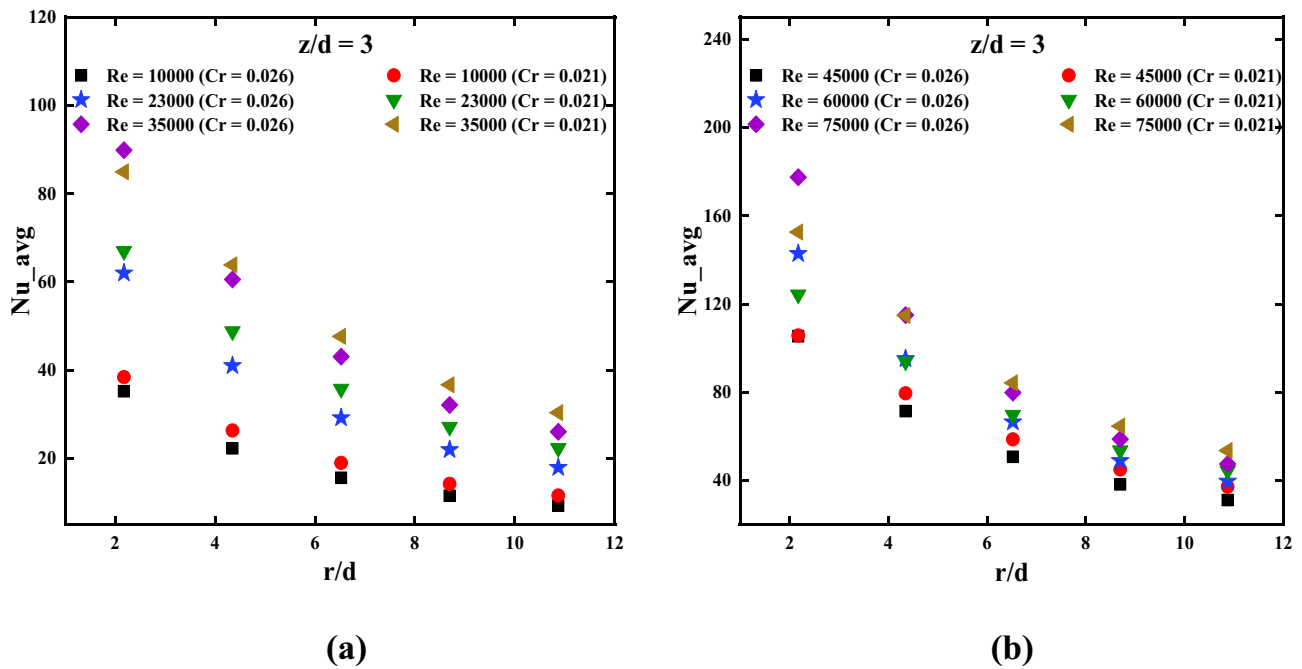**Fig. 9** Effect of variation in Cr on average Nu at different z/d

Fig. 10 Effect of variation in Cr on average Nu at different Re

The impact of Cr on the average Nu by varying the Re is shown in Fig. 10(a, b). The influence of curvature on Nu depends on the region: there is a slight increase in Nu with an increasing curvature ratio for small r/d. However, for larger r/d values, this increase becomes less pronounced. Nu starts decreasing with an increase in Cr. The extent of these two distinct regions is influenced by both Re and z/d. The underlying mechanism for this opposing effect involves two key phenomena. First, the generation of Taylor Görtler vortices enhances turbulence and fluid mixing within the boundary layer, consequently improving heat transfer. Conversely, in the wall jet region, increasing curvature leads to an increase in the boundary layer, which leads to reduced heat transfer. Results show that the Nu variation rises with the rise in Re at radial point directions. This is because a jet with a larger Re brings energy and momentum. At smaller r/d values, Nu is notably high but diminishes as the radial distance increases. Moreover, the influence of the curvature ratio on Nu lessens with an increase in both r/d and Re. At r/d = 10.9, the Nu variation between curvature ratios is about 20% at Re = 10,000, which then decreases to 11% when the mass flow rate is increased to 75,000.

3.7 Comparison of area-average Nu correlation with experimental data

A comparison between the experimental data points for the average Nusselt number and the available correlation

is illustrated in Fig. 11(a)–(c). This comparison is made for various z/d and Re values while maintaining a constant value for Cr at 0.026. Hadipour and Zargarabadi [16] conducted an in-depth analysis of the impact of lower nozzle plate spacing, ranging from 0.1 to 4, on impinging jets acting upon a concave surface. They covered Reynolds numbers between 10,000 and 35,000, maintaining a consistent Cr = 0.1. Their findings, shown in Fig. 11(a), reveal that the data for z/d = 3 fits within the standard deviation range only for Re = 10,000 and 23,000. Intriguingly, experimental data for a jet plate spacing of 6 at Reynolds numbers 10,000 and 23,000, as well as for z/d of 12 at Reynolds number 10,000, align with the + 20% deviation line. However, any other combinations of Re and z/d presented deviations outside the standard range.

Zhou et al. [15] delved into the effects of curvature on jet impingement heat transfer for concave surfaces. They performed experiments for z/d lies between 6 to 12, a Re range of 27,000 to 130,000, and a Cr value between 0.005 and 0.03. Their observations, highlighted in Fig. 11(b), consistently showed that their data points were under-predicted by the correlation, lying outside the expected values.

Fenot et al. [14], in their research, analyzed the heat transfer dynamics of a row of air jets impinging on a concave surface. Their study was constrained to z/d values between 2 and 5, Re from 10,000 to 23,000, and Cr values from 0.1 to 0.2. As seen in Fig. 11(c), experimental data aligns reasonably with the Fenot correlation, especially for z/d values
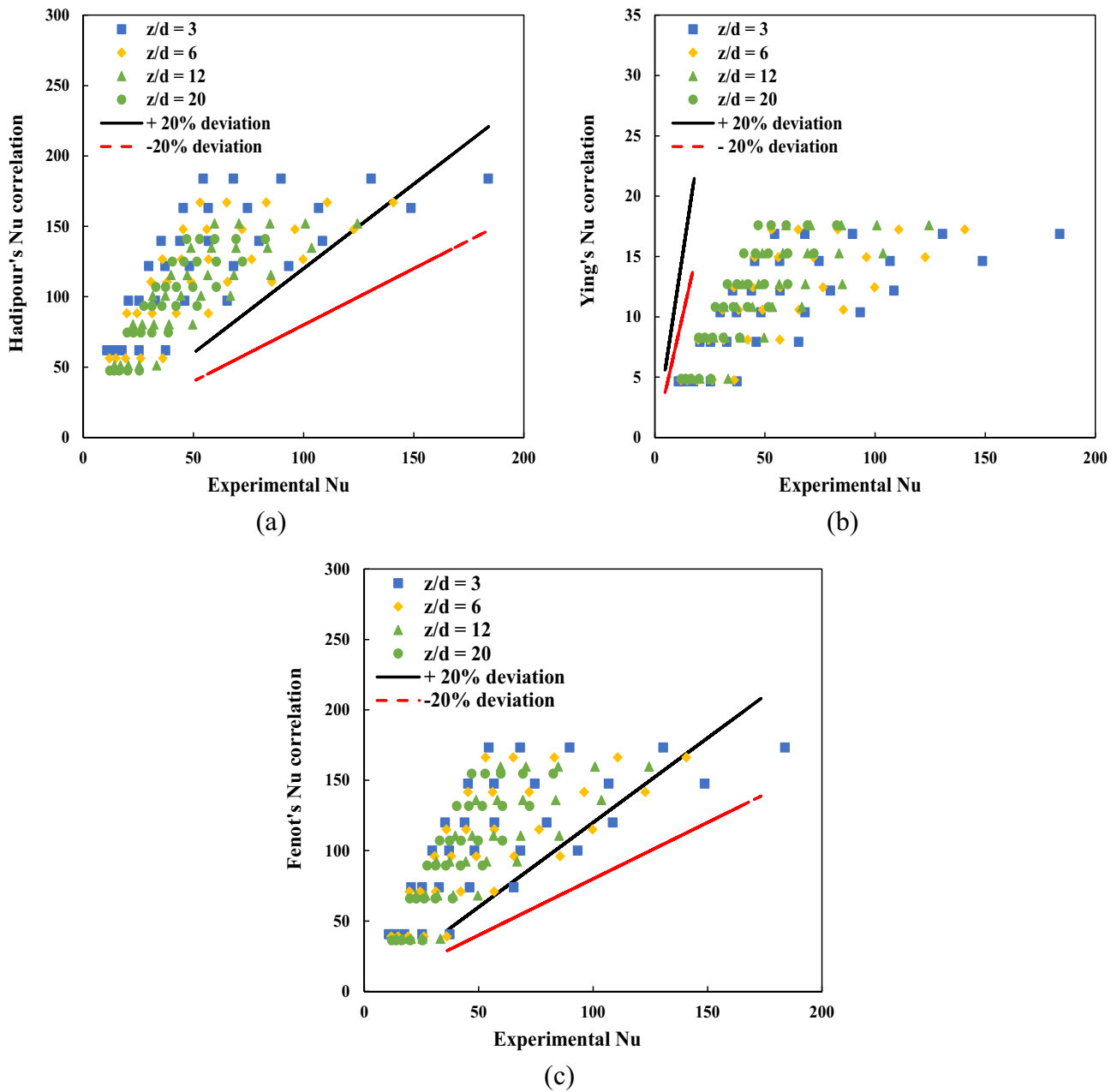
Fig. 11 Comparison of available correlation with the present experimental data

of 3 and 6 within a deviation range of ± 20% for Reynolds numbers between 10,000 and 23,000. However, the correlation over-predicted the remaining data sets.

Thus, it shows that there are some cases where experimental data aligns well with established correlations, there are also several scenarios where deviations—either under-predictions or over-predictions occur, highlighting the complex nature of impinging jet heat transfer on concave surfaces.

3.8 Proposed correlation for area averaged Nusselt number

The average Nusselt number is determined by various geometrical and flow parameters, including the non-dimensional jet-to-plate distance (z/d), radial spacing ratio (r/d), Prandtl number (Pr), curvature ratio (d/D), and Reynolds number (Re). Consequently, the average Nusselt number is expressed as a function of these parameters.

Table 2 Statistical data comparison for average Nusselt number with a proposed and available empirical correlation

Author(s)	MD (%)	MAD (%)	% Data within ± 20% deviation	Deviation range (%)
Hadipour and Zargarabadi [16]	-54.34	54.34	4.17	-82.78 to -0.09
Fenot et al. [14]	123.70	82.46	10	43.51 to 207.99
Zhou et al. [15]	356.18	356.18	0	128.79 to 989.75
Proposed correlation (Eq. 18)	2.75	10.47	100	-22.06 to 35.78

Only three existing correlations are available for predicting the mean Nusselt number. As discussed in Section 3.7, these correlations in Table 2 are applicable within specific ranges of Re and z/d, with none accounting for the influence of r/d. However, when considering the area average, it is essential to account for the plate's area, and thus, r/d is included as a parameter relating to the plate's area. In this current study, the authors have developed a novel correlation capable of predicting the area-averaged heat transfer over a curved surface.

In the present experimental study, Re is varied between 10,000 and 75,000, with a maximum jet-plate spacing of 20d, considered for two different d/D ratios. The radial spacing ratio (r/d) plays a substantial role in influencing heat transfer. This parameter proves to be valuable in determining heat transfer for specific areas or locations

as per specific needs. Therefore, a novel correlation has been developed, incorporating r/d as a function of Re, in addition to Re, Prandtl number (Pr), curvature ratio (d/D), and non-dimensional jet-plate distance (z/d), as illustrated in Eq. (18). It can be confirmed that the newly developed correlation is applicable across the entire range of z/d, r/d, d/D, and Re. The correlation demonstrates good agreement with the experimental data, within ± 20% error, and a mean absolute deviation (MAD) of 10.47%, as illustrated in Fig. 12. A quantitative analysis comparing the experimental data with both the existing and proposed correlations is presented in Table 2. The table provides information on the percentage of MD (mean deviation), the percentage of MAD, the maximum and minimum variations in data, and the percentage of data falling within the maximum deviation range.

Fig. 12 Comparison of experimental area average Nu with the proposed correlation
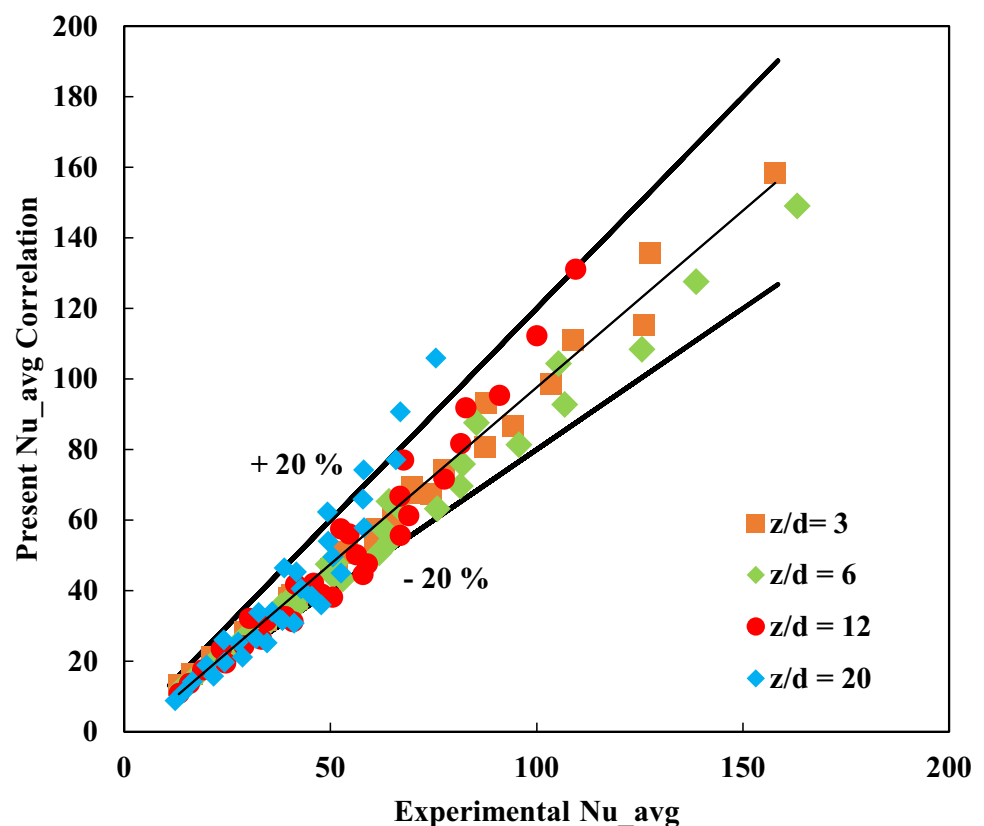
$$Nu_{avg} = 0.158 Re^{0.698} Pr^{0.384} \left(\frac{d}{D} \right)^{0.172} \left[\frac{1.16 - 0.019 \left(\frac{z}{d} \right)}{1 + 0.1 \left(\frac{r}{d} \right)^{1.3}} \right]^{1.1628}$$

$$(18)$$

For $3 \leq z/d \leq 20, 0 \leq r/d \leq 10.87, 10000 \leq Re \leq 75000$

4 Conclusion

The objective of this study is to investigate the area average HTC over a concave surface impacted by an air jet. Several operating conditions were considered, including $10{,}000 \leq Re \leq 75{,}000$, $3 \leq z/d \leq 20$, and $Cr = 0.026$ and 0.021. The results of the current investigation have been presented as follows:

- The maximum Nu is consistently observed for the area near the stagnation region.
- There is a notable decrease in Nu as the distance from the stagnation region increases, particularly towards the edges of the plate in the A5 region.
- The highest area-averaged Nu is observed at $z = 6d$ in the A1 region for $Re = 75{,}000$.
- Nu tends to converge and stabilize in the A4 and A5 regions, indicating a limit to the effectiveness of increasing the plate size for enhancing heat transfer.
- The distribution of area-averaged Nu over different regions on a concave surface show that average Nu increases with increasing Re.
- Nu in circular sections was higher than in square sections at any radial distance. This trend was consistent and became more pronounced with increasing radial distance.
- Circular and square sections provided similar heat transfer rates when they had the same area ratio.
- The area average Nu over the concave surface is a function of the jet Reynold number, jet-to-surface distance, and relative curvature of the impingement surface.
- The influence of the Cr on Nu is significant at small z/d, r/d, and Re.
- It should be noted that for sections having a small radial length, i.e., covering the stagnation and transition region, Nu increases with increasing Cr. Conversely, for the section having the large radial length covering the wall jet region Nu decreases with increasing Cr. The size of these regions is determined by both Re as well as z/d.
- A new empirical correlation for the area-averaged Nu is developed, applicable for all the ranges of Re, z/d, and d/D. The MAD when compared with experimental data is 10.47%.

Data availability No datasets were generated or analysed during the current study.

Declarations

Ethical approval The authors declare that they have adhered to all ethics guidelines mandated by the Journal. The manuscript has been prepared and submitted in accordance with the highest ethical standards, and we assure compliance with Journal guidelines.

Conflict of interest The authors declare no competing interests.

References

1. Sarkar A, Nitin N, Karwe MV, Singh RP (2004) Fluid flow and heat transfer in air jet. J Food Sci 69:113–122
2. Arik M, Sharma R, Lustbader J, He X (2013) Steady and unsteady air impingement heat transfer for electronics cooling applications. J Heat Transfer 135:1–8. https://doi.org/10.1115/1.4024614
3. A Taie AI, Abd HS (2017) Experimental and numerical investigation of impingement cooling of gas turbine combustion chamber liner. J Basic Appl Sci Res 7:17–35
4. Saeed F, Ahmed KZ, Owes AOE, Paraschivoiu I (2021) Anti-icing hot air jet heat transfer augmentation employing inner channels. Adv Mech Eng 13:1–13. https://doi.org/10.1177/16878140211066212
5. Talapati RJ, Katti VV (2023) Local heat transfer characteristics of circular multiple air jet impinging on a semicircular concave surface. Exp Heat Transf 00:1–24. https://doi.org/10.1080/08916152.2023.2209894
6. Alvarez A, Treviño C, Pérez-Flores F, Martínez-Suástegui L (2023) Flow measurements of jet impingement upon a semicylinder with crossflow. Int J Mech Sci 255:108271. https://doi.org/10.1016/j.ijmecsci.2023.108271
7. Yang B, Chang S, Wu H, Zhao Y, Leng M (2017) Experimental and numerical investigation of heat transfer in an array of impingement jets on a concave surface. Appl Therm Eng 127:473–483. https://doi.org/10.1016/j.applthermaleng.2017.07.190
8. Bu X, Peng L, Lin G, Bai L, Wen D (2016) Jet impingement heat transfer on a concave surface in a wing leading edge: Experimental study and correlation development. Exp Therm Fluid Sci 78:199–207. https://doi.org/10.1016/j.expthermflusci.2016.06.006
9. Öztekin E, Aydin O, Avc M (2012) Hydrodynamics of a turbulent slot jet flow impinging on a concave surface. Int Commun Heat Mass Transf 39:1631–1638. https://doi.org/10.1016/j.icheatmasstransfer.2012.10.015
10. Lee DH, Chung YS, Won SY (1999) The effect of concave surface curvature on heat transfer from a fully developed round impinging jet. Int J Heat Mass Transf 42:2489–2497. https://doi.org/10.1016/S0017-9310(98)00318-4

11. Zhou J, Tian J, Lv H, Dong H (2022) Numerical investigation on flow and heat transfer characteristics of single row jet impingement cooling with varying jet diameter. Int J Therm Sci 179:107710. https://doi.org/10.1016/j.ijthermalsci.2022.107710

12. Öztekin E, Aydin O, Avci M (2013) Heat transfer in a turbulent slot jet flow impinging on concave surfaces. Int Commun Heat Mass Transf 44:77–82. https://doi.org/10.1016/j.icheatmasstransfer.2013.03.006

13. Gau C, Chung CM (1991) Surface curvature effect on slot- air-jet impingement cooling flow and heat transfer process. J Heat Transfer 113:858–864. https://doi.org/10.1115/1.2911214

14. Fenot M, Dorignac E, Vullierme JJ (2008) An experimental study on hot round jets impinging a concave surface. Int J Heat Fluid Flow 29:945–956. https://doi.org/10.1016/j.ijheatfluidflow.2008.03.015

15. Zhou Y, Lin G, Bu X, Bai L, Wen D (2017) Experimental study of curvature effects on jet impingement heat transfer on concave surfaces. Chinese J Aeronaut 30:586–594. https://doi.org/10.1016/j.cja.2016.12.032

16. Hadipour A, Rajabi Zargarabadi M (2018) Heat transfer and flow characteristics of impinging jet on a concave surface at small nozzle to surface distances. Appl Therm Eng 138:534–541. https://doi.org/10.1016/j.applthermaleng.2018.04.086

17. Dhruw L, Kothadia H, Kumar A (2022) Investigation of local heat transfer from a flat plate impinged by an inclined circular jet. SSRN Electron J 184:108027. https://doi.org/10.2139/ssrn.4186505

18. Patil VS, Vedula RP (2018) Local heat transfer for jet impingement onto a concave surface including injection nozzle length to diameter and curvature ratio effects. Exp Therm Fluid Sci 92:375–389. https://doi.org/10.1016/j.expthermflusci.2017.08.002

19. Joshi J, Sahu SK (2022) Heat transfer characteristics of flat and concave surfaces by circular and elliptical jet impingement. Exp Heat Transf 35:938–963. https://doi.org/10.1080/08916152.2021.1995082

20. Churchill SW, Chu HHS (1975) Correlating equations for laminar and turbulent free convection from a vertical plate. Int J Heat Mass Transf 18:1323–1329. https://doi.org/10.1016/0017-9310(75)90243-4

21. Kline SJ, Mc Clintock F (1953) Describing uncertainities in single sample. Mech Eng 75:3–8

22. Katti V, Prabhu SV (2008) Experimental study and theoretical analysis of local heat transfer distribution between smooth flat surface and impinging air jet from a circular straight pipe nozzle. Int J Heat Mass Transf 51:4480–4495. https://doi.org/10.1016/j.ijheatmasstransfer.2007.12.024

23. Goldstein RJ (1982) Impingment of a circular jet with and without cross flow. Int J Heat Mass Transf 25:1377–1382